MedCrave
Step into the World of Research
Pharmacy & Pharmacology International Journal

Research Article

Open Access

CrossMark

Physical-mathematical model to predict the kinetic coagulation process by clotting activity of bacterial endopeptidases

Abstract

A physical-mathematical model was used to evaluate the capability of an enzymatic pool of *Bacillus* sp. P7 (isolated from *Piaractus mesopotamicus*) to promote the bovine casein micelles coagulation. Experiments were designed to assess the effects of temperature, pH, and enzyme activity/mass of substrate ratio on the kinetic parameters of the coagulation process and the microstructure of the obtained clots. Descriptive and predictive equations indicate that the temperature and the pH modified these parameters significantly. In optimal conditions, the clot's mean pore size was 3.6 times smaller using chymosin. On the other hand, rheological measurements evidence a moderate elasticity of clot, which indicates the usefulness of P7 protease preparation as a clotting agent in spreadable or soft cheese manufacture. Also, the hydrolysis products, which are in the whey after casein micelles coagulation, demonstrated antioxidant activities. Equations to model and predict the process kinetics were combined with rheological and microstructure analyses of the obtained clots, and whey bioactivities were evaluated. Nevertheless, the use of P7PP requires further investigation concerning the stability of the enzyme preparation during storage, its performance, and how these variables could be related to the proposed models.

Keywords: *Bacillus* sp. P7, bovine casein micelle, enzymatic coagulation, experimental design, antioxidant activity

Volume 10 Issue 4 - 2022

Manuel Mancilla Canales,[1,2] Ana Paula Folmer Corrêa,[3] Bibiana Riquelme,[1,2] Adriano Brandelli,[3] Patricia Risso[2,4]

[1]Grupo de Física Biomédica, Instituto de Física Rosario (CONICET-UNR), Argentina
[2]Facultad de Ciencias Bioquímicas y Farmacéuticas (UNR), Argentina
[3]Instituto de Ciência e Tecnologia de Alimentos, Universidade Federal de Rio Grande do Sul, Brasil
[4]Facultad de Ciencias Veterinarias (UNR), Argentina

Correspondence: Bibiana Riquelme, Grupo de Física Biomédica, Instituto de Física Rosario (CONICET-UNR), 27 de febrero 210bis, 2000 Rosario, Argentina, Tel +54-341-4804593, Email briquel@fbioyf.unr.edu.ar, riquelme@ifir-conicet.gov.ar

Received: August 12, 2022 | **Published:** August 22, 2022

Introduction

Bovine milk proteins are functional food ingredients. Besides their aggregation and coagulation capabilities and functional properties, they have profound economic relevance in the manufacturing of dairy products.[1,2] Gelation or coagulation of CM is one of the most frequently used processes in manufactured dairy products.[3] The enzymes usually used for milk coagulation processes are either acid endopeptidases of animal, plant, or fungal sources; also, they can be obtained by recombinant DNA techniques. Hydrolyzed products obtained with these enzymes may have a bitter taste,[4] making their use without further processing difficult.

Proteolysis has different purposes in the food industry, such as cheese, bakery products, and soy hydrolysates manufacturing, and meat tenderizing.[5,6] Peptides that derive from protein hydrolysis are released during product processing or by gastrointestinal digestion. These possess several biological activities, such as regulatory activities of gastrointestinal, immune, cardiovascular, or nervous systems.[5,7] For this reason, the use of milk protein hydrolysates is potentially significant in the development of new products or food ingredients.

Proteases from microbial sources are of particular interest because of the high yield achieved during their production through well-established culture media. Protease production is an inherent property of microorganisms. The exploitation of its biodiversity is considered a favorable alternative for providing the industry with a great variety of microorganisms and suitable proteases for different purposes.[8] Bacteria from the intestinal tract of fish can be a source of enzyme production.[9] A bacterium isolated from the intestinal tract of *Piaractus mesopotamicus,* phylogenetically identified as *Bacillus,* produces high levels of extracellular proteases when cultured in inexpensive media.[10-12]

These extracellular endopeptidases are active in a range of pH 5-8 and are thermal tolerant to a lesser extent. They generate less bitterness in food protein hydrolysates than acid endopeptidases, making them an alternative for use in the food industry. Their low thermal tolerance could be used for the regulation of their reactivity.[6] Besides, they generate casein hydrolysates with diverse biological activities that are of importance in functional food areas.[13,14]

In foodstuff, protein gels are responsible for most of the rheological and textural properties, such as elasticity, resistance, and hardness.[15] Mechanical properties and texture of the food gel are affected by the initial composition of the system, the interaction between their components, and the conditions during their formation.[16] Changes in the rate of coagulation processes could affect the physical properties of the gel, such as texture and water retention ability. Therefore, the study of the rheological behavior of gels and clots could achieve information about the structure, viscoelasticity, texture, and sensorial characteristics of the final elaborated product.[1]

Image analysis is a valuable tool for the characterization of protein gels.[17,18] This technique allows the understanding of the gel network and how it becomes altered by the elaboration conditions.[19] Textural analysis is one of the main components in image processing as it is an intrinsic property of the surface of objects. The texture of an image refers to parameters like fineness, roughness, smoothness, and granularity. These parameters generally are characterized by the spatial arrangement of gray levels in a given region of the analyzed images.[20]

This work aimed to use a physical-mathematical model to predict the kinetic coagulation process by clotting activity of bacterial endopeptidases. The model was employed to evaluate the proteases from *Bacillus* sp. P7 as a milk-clotting enzyme. An experimental design was performed to determine the significance of the factors involved in the coagulation process, and to establish useful equations

to model and predict the process kinetics. Also, the rheological and microstructure of the obtained clots and whey bioactivities were evaluated.

Materials and methods

Protease production

The enzymatic pool was obtained from the *Bacillus* sp. P7 strain isolated from the intestine of the fish *Piaractus mesopotamicus.*[13] In brief, the growing medium was principally chicken feather meal at 10 g L^{-1} (0.5 g L^{-1} NaCl, 0.4 g L^{-1} KH_2PO_4, 0.3 g L^{-1} K_2HPO_4 and 10 g L^{-1} chicken feather meal). The partial purification was carried out by centrifugation at 3,000 g, precipitation with ammonium sulfate at 60% saturation, and chromatography in a Sephadex G-100 (Pharmacia Biotech, Uppsala, Sweden) gel filtration column.

Proteolytic activity assay

Proteolytic activity was determined using azocasein as substrate as described by Hummel[21] with minor modifications. The reaction mixture (0.3 mL) was prepared with 0.1 mL of P7 protease, 0.1 mL of 0.02 M Tris-HCl buffer pH 8, and 0.1 mL of 10 g L^{-1} azocasein (Sigma-Aldrich, Argentina) in Tris-HCl buffer. A volume of 0.5 mL of 100 g L^{-1} trichloroacetic acid (TCA) was used to stop the reaction after an incubation period of 10 min at 37ºC. Centrifugation was carried out at 10,000 g for 5 min. The supernatant obtained was mixed with 0.2 mL of 1.8 M NaOH and the absorbance of the reaction mixture was determined at 420 nm. One proteolytic activity unity (U) was defined as the amount of protease able to increase absorbance in 0.1 units under such conditions. Fractions showing proteolytic activity on azocasein were recollected and named hereafter as a P7 protease preparation (P7PP).

Casein micelle suspensions

CM were reconstituted from skimmed bovine milk powder (Svelty, Nestlé, Argentina) at 10 % (w/v) in an aqueous solution of 0.01 M calcium chloride with 0.01 M Tris-HCl buffer (pH set at 6.5 or 8.5). Protein concentration was analyzed by spectrometry, where a modification of the tyrosine amino acid spectrum at higher wavelengths from the UV region in a strongly alkaline medium (pH □13) was performed.[22]

CM aggregation

The kinetics of CM aggregation induced by P7PP was evaluated through turbidity measurements as a function of time. Changes in the average size of colloidal particles (and/or the compactness degree of the aggregates) obtained at the end of the process were determined as previously explained[23] by the changes in turbidity (τ) as a function of wavelength (λ) in the 450-650 nm range, where there was no absorption of protein chromophore groups. The parameter β is related to the average size and the compactness degree of particles:

$$\beta = 4.2 + \frac{\partial \log(\tau)}{\partial \log(\lambda)} \quad (1)$$

Where $\partial\log(\tau)/\partial\log(\lambda)$ is the slope of a lineal log(τ) versus log(λ) plot.[24] This plot could be obtained from absorption spectra at different times before and during the aggregation process. Therefore, in the coagulation process, β can be used to evaluate the status of the particles. Fractal dimension (D_f) measure of compactness degree of the clot network and is the maximum value achieved by β.[25-27] The initial aggregation rate (v_i) was estimated as the slope of the initial linear section in a plot of β versus time. The time when the aggregation process begins was referred to as t_{ag}, which was the time to occurring a sudden rise in β values. These determinations were carried out using a spectrophotometer (Spekol 1200, Analytikjena, Belgium) with a diode arrangement.

Previous analyses for characterization of P7PP as pH and temperature (*T*) stability assays led to the consideration of how pH, *T*, and enzyme activity/substrate mass ratio (*E/S*) affect the aggregation process induced by P7PP. The process could be characterized by t_{ag}, v_i, and D_f parameters.

A 2^3 factorial experimental design was performed to evaluate the effect of the factors involved in the enzymatic aggregation process.[28] For this, *E/S*, *T*, and pH were considered independent factors. The assays were initiated by adding the required P7PP volume, keeping casein and calcium concentrations constant (30 g L^{-1} and 0.01 M, respectively), and were replicated twice. Response variables were t_{ag}, v_i, and D_f. Statistically significant factors and interactions were determined with the corresponding analysis of variance (ANOVA). Residuals were analyzed to check the validity of the assumptions (constant variance, normality, and independence of residuals). Response variables were fitted with codified variables to achieve descriptive and predictive mathematical models for the system. Optimum values of pH, *T*, and *E/S* were determined individually for each response variable, considering how t_{ag}, v_i, and D_f were related to the factors under study.

Determination of the P7PP clotting activity

P7PP clotting activity (*CA*) on the CM was determined using a method based on the visual evaluation of the appearance of the first clot.[29] For this method, a 100 µL volume of P7PP at 7U was added to 2 mL of CM suspension with a concentration of 30 g L^{-1} in 0.01 M Tris-HCl buffer, and 0.01 M calcium chloride at the desired pH. The pH was 6.4, 7.4 or 8.4, and the incubation temperature was 34, 44 or 55°C. The time elapsed from the coagulant addition until the occurrence of the first clots (coagulation time, t_c) was registered. P7PP clotting activity on the MC unity (U_{CA}) was defined as the amount of enzyme in 1 mL necessary to coagulate 1 mL of MC in 2,400 s.

$$CA\left(U_{CA}/mL\right) = \frac{2{,}400}{t_c} \cdot \frac{V_{CM}}{V_{P7PP}} \quad (2)$$

where V_{CM} is the volume of CM suspension and V_{P7PP} is the volume of P7PP.

Conventional optical microscopy

The microstructure of the resulting clots by the addition of P7PP to CM suspension was evaluated by conventional optical microscopy. A sample volume of 0.09 mL was deposited in LAB-TEK II cell compartments (Sigma-Aldrich, Argentina), which were placed in an oven at (44±1)°C temperature with controlling humidity during the coagulation process. The clots were observed with an oil immersion objective of 100x on an inverted microscope (Union Optical, Tokyo, Japan) coupled to a digital camera (Canon Powershot A640, Tokyo, Japan) with a 52 mm adaptor and 7.1x Zoom. The acquired images were stored for further analysis.

Average pore size

The mean diameter of pores or interstices of the clots, obtained by adding the P7PP to CM suspension, was determined through ImageJ software analysis. It was determined that 1 pixel = (0.0399±0.0001) µm using a micrometric rule. Then, the image resolution in this optical system was 25.0 pixels/µm.

Citation: Mancilla Canales M, Folmer Corrêa AP, Riquelme B, et al. Physical-mathematical model to predict the kinetic coagulation process by clotting activity of bacterial endopeptidases. *Pharm Pharmacol Int J.* 2022;10(4):130–137. DOI: 10.15406/ppij.2022.10.00375

Textural analysis of images

The images obtained by conventional optical microscopy were analyzed using textural parameters. Two estimators were calculated using a specific algorithm written in Python language developed by H. Castellini for this purpose.[17,18] The estimators were the Shannon entropy (*S*) and the Uniformity (*Y*),[20,30] defined as follow:

$$S = -\sum_{i=0}^{L-1} p(N_i).\log_2\left(p\left(N_i\right)\right) \quad (3)$$

$$Y = \sum_{i=0}^{L-1} p^2(N_i) \quad (4)$$

where p(N_i) is the sample statistical frequency of gray scales and L is the maximum level of black achieved.

In an image that presents all gray levels values (0 to 255) with equal occurrence/representation (maximally uniform), Y takes its maximal value and decreases from thereafter. In contrast, *S* measures the variability of the intensity in the gray level distribution, being maximal for an image that contains all the shades of gray with equal probability. Consequently, a high *S* value and a small *Y* value correspond to structures those the component particles are in well-defined sectors. On the other hand, a small *S* value and a high *Y* value correspond to structures with particles dispersed throughout their volume.[24]

Rheological assays

The kinetics of CM coagulation was evaluated through dynamic rheological experiments with stress- and strain-controlled rheometer using a cone/plate geometry (diameter: 40 mm; cone angle: 2º; cone truncation: 55 mm; TA Instruments, AR G2 model, USA). A solvent trap cover was utilized to avoid the contraction of the sample by water evaporation. The temperature was controlled with a recirculation bath connected to the Peltier plate of the instrument. Coagulation time (t_c) was considered as the time in which elastic modulus (*G'*) and viscous modulus (*G"*) become equal. According to the criterion adopted by several authors to study the protein gelation, the maximal *G'* value achieved (*G'max*) was recorded to characterize the system and to provide a reference for comparison.[31-33] Measurements were performed every 30 s with constant oscillation stress of 0.1 Pa and at 0.1 Hz. A frequency scan between 0.1 and 10 Hz was performed when the equilibrium was reached.

Whey bioactivities *in vitro*

Serum samples obtained after P7PP enzymatic action (7 U) at pH 7.4 and 44°C (optimum conditions) were lyophilized for further their antioxidant capacity study. The scavenging of the 2,2′-azino-bis-(3-ethylbenzothiazoline)-6-sulfonic acid (ABTS) radical and the reducing power of whey samples were determined. Scavenging of the ABTS radical was determined by the decolorization assay described by Re *et al*.[34] and Folmer Corrêa *et al*.[35] Briefly, a solution of ABTS radical cation ($ABTS^{\bullet+}$) was prepared by reacting 7 mM ABTS solution with 0.14 M K_2SO_4 (final concentration). For the assay, the $ABTS^{\bullet+}$ was diluted with 5 mM phosphate-buffered saline pH 7.0 (PBS) to an absorbance of 0.70±0.02 at 734 nm. A 10 µL (15 g L^{-1}) sample was mixed with 1 mL of diluted $ABTS^{\bullet+}$ to measure the absorbance at 734 nm (A_S) after 6 minutes.

Then, the percentage inhibition was calculated as:

$$\text{Scavenging activity}(\%) = (1 - \frac{A_s}{A_0}) \cdot 100 \quad (5)$$

where A_0 is the absorbance of the reaction mixture without whey samples.

The reducing power of the whey samples was measured as previously reported by Oyaizu,[36] which is based on the ability of the sample to reduce the Fe^{3+}/ferricyanide complex to the ferrous form. Briefly, a volume (2.5 mL) of whey samples (5, 10, 15, and 20 g L^{-1}) was mixed with 2.5 mL of 0.2 M phosphate buffer pH 6.6 and 2.5 mL of 10 g L^{-1} potassium ferricyanide. Then, the mixture was incubated at 50ºC for 20 min. After that, 2.5 mL of 0.10 g mL^{-1} TCA was added, and the mixture was centrifuged (3,000 g for 10 min). Equal volumes (2.5 mL) of supernatant and distilled water were mixed, 0.5 mL of 1 g L^{-1} ferric chloride was added, and the absorbance at 700 nm was measured. The higher absorbance of the reaction mixture indicated a greater reducing power. Butylated hydroxytoluene (BHT) was used as a positive control.[37]

Statistical analysis

Measurements were performed at least in duplicate. Results were reported as mean values ± standard error. Statistical analysis was performed with Sigma Plot 10.0 and Minitab 16 software. ANOVA was used to determine significant differences ($p < 0.05$) between variables.

Results and discussion

Evaluation of CM aggregation induced by P7PP

P7PP capability to induce colloidal destabilization of CM and their subsequent aggregation was evaluated using an experimental design. Table 1 shows the values of the independent variables assayed (pH, *T*, *E/S*) and the response variables (t_{ag}, v_i, and D_f) obtained during the post enzymatic aggregation of CM. Table 2 shows the coefficients and *p*-values obtained in coded units for the response variables. For t_{ag}, from the ANOVA of the responses studied in the experimental design (Table 2), all the independent variables (*T*, pH, and *E/S*) and their interactions (pH**T*, pH**E/S*, and *T***E/S*) were significant ($p < 0.05$) as shown in Equation 6.

$$t_{ag} = 3.88 + 2.40\,pH - 2.37T - 2.48E/S - 0.90\,\text{pH*T} - 1.74\,\text{pH*E/S} + 1.45\,\text{T*E/S} \quad (6)$$

When pH decrease, CM negative surface charge density decrease, and the electrostatic stability diminish. Therefore, an enhancement in the aggregation process would occur (lower t_{ag}). As T increase, the rate of the processes leading to coagulation enhances. Also, an increase in *E/S* represents an increase in the protein hydrolysis rate and, consequently, a decrease in the time needed for destabilization of CM particles, which then start to aggregate. Figure 1 shows the corresponding response surface plot obtained.

All the independent variables were statistically significant ($p<0.05$) for v_i, and Equation 7 contains the calculated coded mathematical model for the variation of this variable, which was obtained through the response surface (Figure 2).

$$v_i = 0.1631 - 0.0353\,pH + 0.0496T + 0.0772E/S - 0.0147\,pH*E/S + 0.0197T*E/S \quad (7)$$

Equation 7 analysis shows that the factor level combination that yields higher v_i values was the same as the one which led to smaller t_{ag} values. Consequently, independent variables acting over v_i produce opposite effects over t_{ag}. Thus, these observations suggest that changes in *T*, pH, and *E/S* led to a decrease in *tag* increasing v_i. Only pH and T independent variables and their interaction were found to be significant ($p < 0.05$) for D_f. Figure 3 shows the response surface plot obtained, and Equation 8 describes the calculated coded mathematical model.

$$D_f = 2.465 - 0.207\,pH + 0.089T - 0.043\,pH*T \quad (8)$$

Citation: Mancilla Canales M, Folmer Corrêa AP, Riquelme B, et al. Physical-mathematical model to predict the kinetic coagulation process by clotting activity of bacterial endopeptidases. *Pharm Pharmacol Int J.* 2022;10(4):130–137. DOI: 10.15406/ppij.2022.10.00375

Table 1 Aggregation time (*tag*), the initial rate of aggregation (*vi*), and fractal dimension (*Df*) as a function of pH, temperature (*T*), and enzyme activity per substrate mass (*E/S*) values used in the experimental design, with the respective coded values in parenthesis

Independent variables			Response variables					
			t_{ag} (min)		v_i (min^{-1})		D_f	
pH[a]	*T* (°C)[a]	*E/S* (Ug^{-1})[a]	Original	Duplicate	Original	Duplicate	Original	Duplicate
6.5 (-1)	40 (-1)	38.89 (+1)	1.412	1.504	0.207	0.242	2.429	2.452
8.5 (+1)	40 (-1)	38.89 (+1)	3.494	2.87	0.118	0.117	2.194	2.205
6.5 (-1)	55 (+1)	38.89 (+1)	0.000[b]	0.000[b]	0.355	0.357	2.834	2.835
8.5 (+1)	55 (+1)	38.89 (+1)	0.902	0.966	0.247	0.279	2.262	2.257
6.5 (-1)	40 (-1)	9.72 (-1)	5.137	3.752	0.075	0.079	2.618	2.66
8.5 (+1)	40 (-1)	9.72 (-1)	15.245	16.584	0.034	0.036	2.21	2.245
6.5 (-1)	55 (+1)	9.72 (-1)	0.000[b]	0.000[b]	0.121	0.151	2.771	2.777
8.5 (+1)	55 (+1)	9.72 (-1)	5.066	5.097	0.094	0.097	2.368	2.329

[a]coded value in parenthesis

[b]too low to be measured

Table 2 Analysis of the coefficients (in coded units) and p-values of the responses aggregation time (*tag*), the initial rate of aggregation (*vi*), and fractal dimensions (*Df*)

Source	t_{ag}(min)		v_i(min^{-1})		D_f	
	Coefficient	*p*-value	Coefficient	*p*-value	Coefficient	*p*-value
constant	3.877	–[a]	0.16306	–[a]	2.4654	–[a]
pH	2.401	–[a]	-0.03531	–[a]	-0.2067	–[a]
T	-2.373	–[a]	0.04956	–[a]	0.0889	–[a]
E/S	-2.483	–[a]	0.07719	–[a]	-0.032	–[b]
pH*T	-0.897	–[a]	0.00194	–[b]	-0.0434	–[a]
pH*E/S	-1.737	–[a]	-0.01469	–[a]	0.0027	–[b]
T*E/S	1.446	–[a]	0.01969	–[a]	0.0246	–[b]

[a]significant ($p < 0.05$)

[b]not significant ($p > 0.05$)

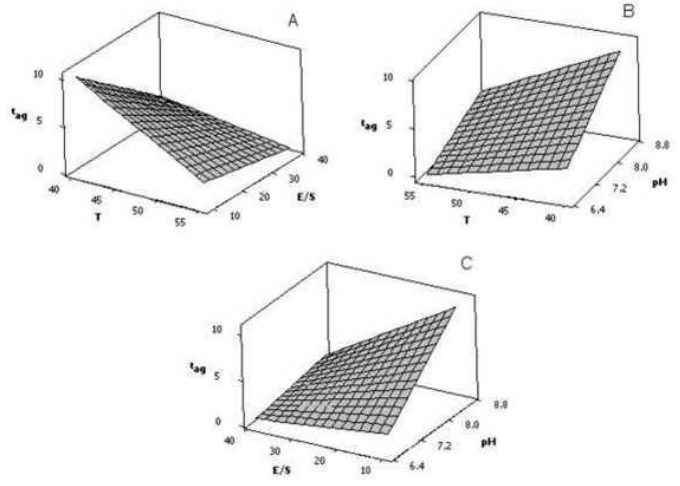

Figure 1 Response surface plot for aggregation time (*tag*) evaluated at CM aggregation induced by P7PP (CM 30 g.L^{-1}, P7PP 7 U). **(A)** *tag* versus substrate mass (*E/S*) values and temperature (*T*), **(B)** *tag* versus pH and *T*, **(C)** *tag* versus pH and *E/S*.

According to the model shown in Equation 8, the compactness degrees of the obtained aggregates were independent of the amount of enzyme added. As mentioned above, a pH decrease promotes CM aggregation and, therefore, more compact aggregates. *T* variations produce two opposite effects. On the one hand, an increment in *T* favors the establishment of hydrophobic interactions (positive enthalpy variation) involved in the bond strengthening, and/or local rearrangements of the clot network. On the other hand, an increase in *T* promotes a decrease in t_{ag}; thus, the rearrangements of the interactions into the gel network are limited, and clots which take longer to form would be more compact.

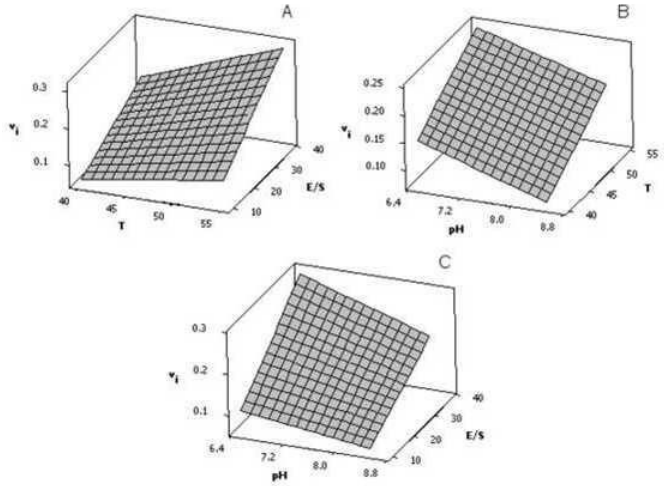

Figure 2 Response surface plot for the initial rate of aggregation (*vi*) evaluated at CM aggregation induced by P7PP (CM 30 g.L^{-1}, P7PP 7 U). **(A)** *vi* versus substrate mass (*E/S*) values and temperature (*T*), **(B)** *vi* versus pH and *T*, **(C)** *vi* versus pH and *E/S*.

P7PP clotting activity

The effect of pH and *T* on the P7PP *CA* was assessed after verifying by turbidimetry that P7PP promotes the colloidal destabilization and subsequent aggregation of CM. For this, a 3^2 factorial experimental design was performed (Table 3). With the same trends as for v_i and D_f, it was determined that pH ($p = 0.038$) and *T* ($p = 0.039$) significantly affected P7PP *CA*. However, no interaction between pH and *T* factors

Citation: Mancilla Canales M, Folmer Corrêa AP, Riquelme B, et al. Physical-mathematical model to predict the kinetic coagulation process by clotting activity of bacterial endopeptidases. *Pharm Pharmacol Int J.* 2022;10(4):130–137. DOI: 10.15406/ppij.2022.10.00375

was observed ($p > 0.05$) at the assayed micelle concentration and amount of P7PP. Equation 9 shows the calculated coded mathematical model for the variation of P7PP *CA*.

$$CA = 488 - 71.1\,pH + 6.96T \quad (9)$$

The clotting activity is expected to increase by ~7 UCA mL^{-1} for each unit increase of *T* within the tested ranges of pH (6.4 to 8.4) and *T* (34°C to 54°C) as long as the pH remains constant. As *T* rises, the coagulation rate increases, and hydrophobic interactions are enhanced. If *T* is kept constant, for each 0.1 increase of pH, the clotting activity is expected to decrease in ~7 UCA mL^{-1}. When pH rises, CM negative surface charge density increases, and the electrostatic stability decreases (higher v_i, lower t_{ag}); therefore, the clotting activity diminishes.

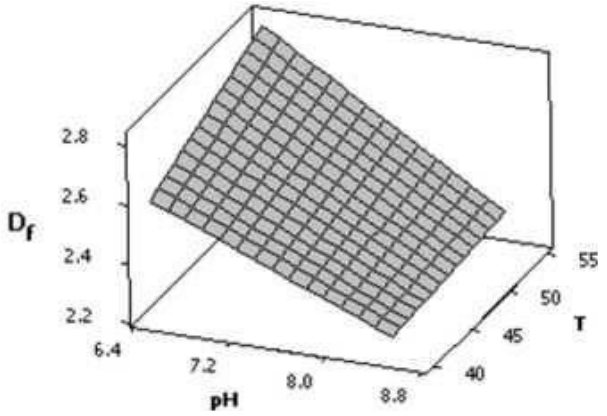

Figure 3 Response surface plot for fractal dimensions (*Df*) evaluated at CM aggregation induced by P7PP (CM 30 $g.L^{-1}$, P7PP 7 U). *Df* versus pH and temperature (*T*).

Evaluation of clots microstructure

After the addition of P7PP to CM suspensions, digital images of clots were registered. Figure 4 shows an example of such images. A protein network (white pixels) is observed identifying the interstices or pores (black pixels). The digital images obtained for all the assessed conditions (Table 3) were used to evaluate the microstructure of the clots through the determination of the pore size distributions and mean pore sizes (Figure 5).

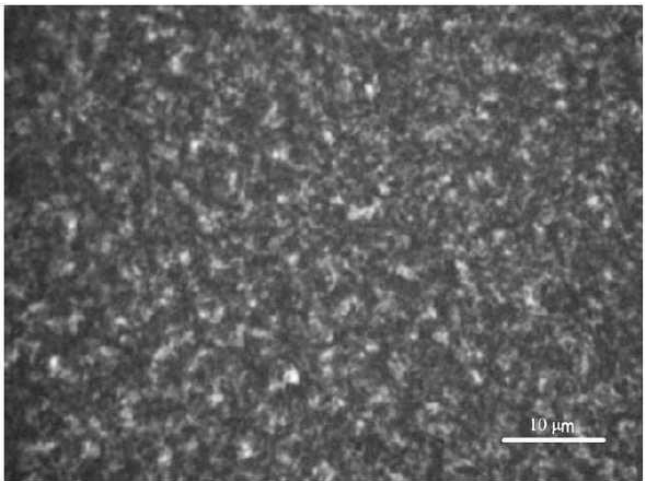

Figure 4 Example of a digital image of clot microstructure obtained at pH 6.4 and a temperature of 34°C after the addition of P7PP to CM suspensions. Image resolution: 25.0 pixel/µm.

Table 3 P7PP clotting activity on the MC (U_{CA} mL^{-1}) as a function of pH and temperature (*T*) values used in the experimental design, with the respective coded values in parenthesis

Independent variables		Response variable
pH[a]	*T*(°C)[a]	*CA* (U_{CA} mL^{-1})
6.4 (-1)	34 (-1)	266.7
7.4 (0)	34 (-1)	266.7
8.4 (+1)	34 (-1)	144.9
6.4 (-1)	44 (0)	266.7
7.4 (0)	44 (0)	266.7
8.4 (+1)	44 (0)	114.3
6.4 (-1)	54 (+1)	381
7.4 (0)	54 (+1)	500
8.4 (+1)	54 (+1)	228.6

[a]coded value in parenthesis

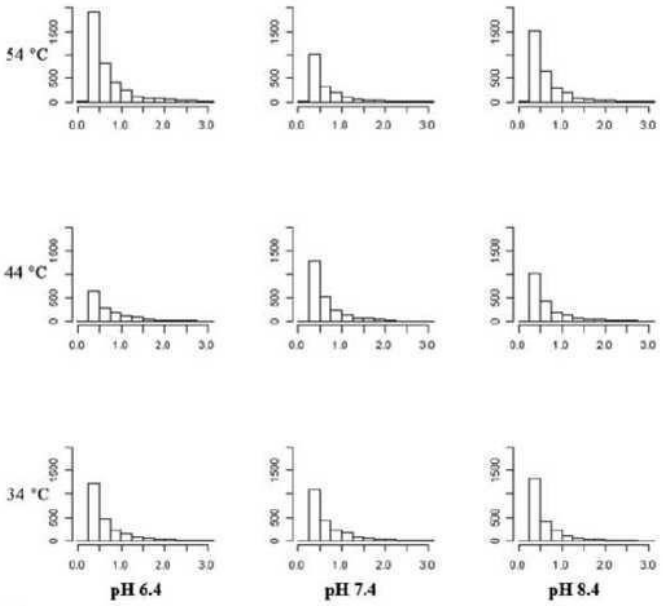

Figure 5 Pore size distribution at pH (6.4, 7.4, 8.4) and *T* (34°C, 44°C, 54°C) after the addition of P7PP to CM suspensions (CM 30 $g.L^{-1}$, P7PP 7 U).

In general, changes in the pore size distribution and a higher number of smaller pores were observed for high *T* values and low pH. As expected, and in agreement with the opposite effects of *T* and pH on P7PP *CA*, marked differences in the pore size distribution at pH 8.4 and 34°C (high pH and low *T*, low *CA*) compared with pH 6.4 and 54°C (low pH and high *T*, high *CA*) were observed. Figure 5 shows an increase of ~80% in the number of smaller pores when moving from low to high *CA*. That is, the microstructure of clots might be related to P7PP *CA*. Low P7PP *CA* promotes the formation of a protein network with relatively large pores. High P7PP *CA* leads to clot formation with a smaller average interstices size, i.e., a clot with a more compact protein network (higher D_f).

From the textural analysis of digital images, descriptive and predictive model equations of the texture of clots under the pH and *T* conditions described in Table 3 can also be obtained. A 3^2 factorial experimental design was performed, and nine images were taken for each experimental condition. Textural parameters (*S* and *Y*) of the corresponding images obtained by optical microscopy were calculated. For both parameters, *T* and pH were statistically significant ($p < 0.05$). In both cases, no interaction between pH and *T* factors was observed ($p > 0.05$).

Citation: Mancilla Canales M, Folmer Corrêa AP, Riquelme B, et al. Physical-mathematical model to predict the kinetic coagulation process by clotting activity of bacterial endopeptidases. *Pharm Pharmacol Int J.* 2022;10(4):130–137. DOI: 10.15406/ppij.2022.10.00375

Equation 10 shows the calculated coded mathematical model for the variation of *S*. It was observed that pH (p=0.001) and *T* (p=0,012) significantly affect this textural parameter.

$$S = 6.24 + 0.0065\,pH - 0.133T \quad (10)$$

On the other hand, Equation 11 shows the mathematical model in coded variables for the variation in *Y*. It was observed that pH (p = 0.004) and *T* (p = 0.001) significantly influence this textural parameter.

$$Y = 16.6 \cdot 10^{-3} - 0.455 \cdot 10^{-3}\,pH + 2.17 \cdot 10^{-3} T \quad (11)$$

By increasing *T* and diminishing the pH, *Y* enhances, and *S* decreases. High values of *Y* and low values of *S* are related to particles localized in well-defined sectors. On the contrary, low *T* and high pH values lead to a decrease in *Y*, and to an increase in *S*, corresponding to irregular arrangements. In addition, since an increase in *T* leads to more structured clots, it can be inferred that hydrophobic interactions are mainly involved in clot formation.

Multi-response analysis

In the food industry, it is often desirable to obtain higher consistency of milk clots. Enzymes like calf rennet have been used in combination with high-pressure homogenization procedures to improve the cheese manufacturing process and the quality of the product.[38]

The coagulation process should not be carried out rapidly to obtain more consistent clots because, if so, less structured clots are obtained (low D_f).[25] Joint consideration of t_{ag} and D_f response variables in the evaluated region was undertaken to optimize the enzymatic coagulation process. It is desirable to have a maximal D_f value to obtain a compact dairy product. If v_i is too high (t_{ag} too low), the rearrangements of the interactions into the clot network are limited, leading to less compact clots. In addition, it is convenient to employ a small amount of P7PP to manufacture a less expensive product.

The models for D_f and t_{ag} presented stationary points in the operated region and when considering the models together, the conditions of pH = 7.4 and T = 44°C were found to be optimal to maximize both variables. In these optimal conditions, the mean pore size assumes a value of (1.54±0.04) µm, 3.6 times minor than when chymosin was used as a clotting agent (5.50±0.03) µm. On the other hand, mean values for the textural parameters obtained for P7PP (S = 6.3±0.1; Y = 0.015±0.002) and chymosin (S = 6.1±0.2; Y = 0.017±0.002) were similar.

Rheological measurements

Rheological properties were evaluated during CM coagulation induced by P7PP at optimal conditions (pH 7.4, T 44ºC). Variations of elastic modulus (*G'*) and viscous modulus (*G"*) as a function of time are shown in Figure 6. A slow stage where both moduli have low values indicating that samples mainly had a viscous behavior during the CM coagulation process. This stage was followed by a sharp increment in both moduli (especially of *G'*), which indicates that the samples present an elastic behavior. These two stages would describe the initial formation of the gel network and subsequent bond strengthening and/or local rearrangements that contribute to clot stiffness degree.

Mean values of t_c and *G'max* were (8.32±0.01) min and (13.0±0.2) Pa, respectively. Other authors, who use chymosin as a clotting agent, reported the same profiles.[1,2,39] Figure 7A shows *G'* and *G"* as a function of the oscillation frequency for the CM coagulation process by the action of P7PP. It was observed that *G'* values were above *G"* values in all the frequency ranges studied. Therefore, the behavior of the elastic component suggested that the samples behaved as elastic solids in the frequency region evaluated. The increase in *G'* values could be attributed to casein particle fusion by rearrangements of inter- and intra- molecular interactions of the achieved clots.[2] Figure 7B shows loss tangent (tan δ=*G"/G'*) as a function of oscillation frequency. An increase in this parameter indicates an increase in the fluidity of the sample when the frequency is increased.[1] The moderate clot elasticity obtained can be the basis for the manufacture of soft cheeses and spreads.

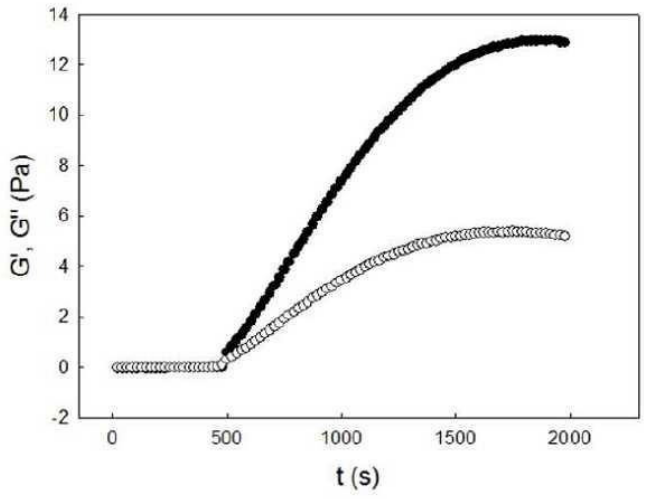

Figure 6 Elastic modulus (*G'*) and viscous modulus (*G"*) as a function of time for the CM coagulation process by the action of P7PP (pH 7.4, 44°C, CM 30 g.L^{-1}, P7PP 7 U).

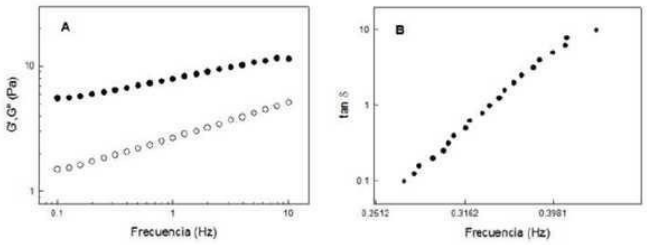

Figure 7 Rheological results for the CM coagulation process by the action of P7PP (pH 7.4, 44°C, CM 30 g.L^{-1}, P7PP 7 U) (A) *G'* and *G"* as a function of the oscillation frequency, (B) loss tangent (tan δ=*G"/G'*) as a function of oscillation frequency.

Whey bioactivities

Peptides with various bioactivities in dairy products such as different cheese varieties and fermented milk have been reported.[40-43] In the whey obtained after the action of P7PP (pH 7.4, *T* 44ºC), scavenging activity of ABTS$^{\bullet+}$ (%) of (19.77±1.49) was determined. A calibration curve with ascorbic acid was performed, and it was determined that such antioxidant capacity was equivalent at concentrations of 0.56 mM ascorbic acid. Hernández-Ledesma et al.[44] also reported ABTS$^{\bullet+}$ radical- scavenging capacity of commercial fermented milk.

Whey samples proved to have the capability to reduce the Fe^{3+}/ferricyanide complex to the ferrous form. A linear increment of the absorbance at 700 nm as the whey concentration increased was observed (Figure 8). Peptides in serum would act as reducing agents by mean of the electron donation, which lead to the formation of more stable products.[45]

Citation: Mancilla Canales M, Folmer Corrêa AP, Riquelme B, et al. Physical-mathematical model to predict the kinetic coagulation process by clotting activity of bacterial endopeptidases. *Pharm Pharmacol Int J.* 2022;10(4):130–137. DOI: 10.15406/ppij.2022.10.00375

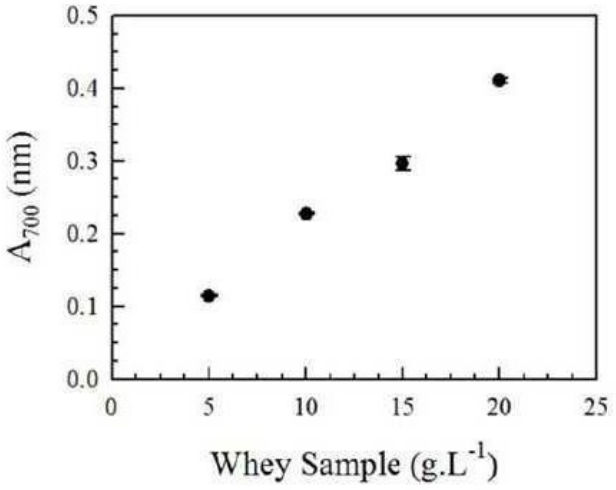

Figure 8 Reduction of Fe^{3+}/ferricyanide complex to the ferrous form by whey product obtained after the action of P7PP (pH 7.4, 44°C, CM 30 g.L^{-1} P7PP 7 U). (Absorbance at 700 nm).

Conclusion

In conclusion, the enzymatic pool obtained from *Bacillus* sp. P7 strain-induced casein micelles coagulation. It was possible to attain equations useful to model and predict the kinetics of this coagulation process and the textural characteristics of the obtained clots. Changes in *T* and pH modified the microstructure of clots. The hydrolysis products, which are in the whey after casein micelles coagulation, demonstrated antioxidant activities. This fact would allow the use of whey, which is generally regarded as industrial waste, and turn it into a potential ingredient for functional foods. The results obtained in this work represent an evaluation and an optimization of the conditions for the utilization of P7PP as a clotting enzyme using a physical-mathematical model, which could be used to predict the kinetic coagulation process. Equations to model and predict the process kinetics were combined with rheological and microstructure analyses of the obtained clots, and whey bioactivities were evaluated. Nevertheless, the use of P7PP requires further investigation concerning the stability of the enzyme preparation during storage, its performance, and how these variables could be related to the proposed models.

Funding sources

This work was financially supported by Universidad Nacional de Rosario, Agencia Nacional de Promoción Científica y Tecnológica (PICT-2011-1354), the Cooperation Program between Coordenação de Aperfeiçoamento de Pessoal de Nível Superior (CAPES) from Brazil and the Ministerio de Ciencia, Tecnología e Innovación Productiva (MINCyT) from Argentina. Manuel Mancilla Canales was research fellow of Consejo Nacional de Investigaciones Científicas y Técnicas (CONICET), Argentina.

Acknowledgments

The authors thank Ana Apesteguía and Renata Aline dos Santos da Fonseca for their contribution to part of the laboratory determinations.

Conflicts of interest

Authors declare that there is no conflict of interest.

References

1. Lucey JA. Formation and Physical Properties of Milk Protein Gels. *Journal of Dairy Science*. 2002;85(2):281–294.
2. Mellema M, Walstra P, Vliet T, et al. Effects of structural rearrangements on the rheology of rennet- induced casein particle gels. *Advances in Colloid and Interface Science*. 2002;98(1):25–50.
3. Walstra P, Jenness R. *Dairy chemistry and physics*. New York, USA: John Wiley & Sons; 1984.
4. Singh TK, Young ND, Drake MA, et al. Production and Sensory Characterization of a Bitter Peptide from β-Casein. *J Agri Food Chem*. 2005;53(4):1185–1189.
5. Alagarsamy S, Larroche C, Pandey A. Microbiology and industrial biotechnology of food-grade proteases: a perspective. *Food Technology and Biotechnology*. 2006;44(2):211.
6. Kasana RC, Salwan R, Yadav SK. Microbial proteases: detection, production, and genetic improvement. *Crit Rev Microbiol*. 2011;37(3):262–276.
7. Korhonen H, Pihlanto A. Bioactive peptides: Production and functionality. *International Dairy Journal*. 2006;16(9):945–960.
8. Razzaq A, Shamsi S, Ali A, et al. Microbial proteases applications. *Frontiers in Bioengineering and Biotechnology*. 2019;7:110.
9. Esakkiraj P, Immanuel G, Sowmya SM, et al. Evaluation of protease-producing ability of fish gut isolate Bacillus cereus for aqua feed. *Food and Bioprocess Technology*. 2009;2(4):383–390.
10. Giongo J, Lucas FS, Casarin F, et al. Keratinolytic proteases of Bacillus species isolated from the Amazon basin showing remarkable de-hairing activity. *World Journal of Microbiology and Biotechnology*. 2007;23(3):375–382.
11. Daroit DJ, Correa AP, Brandelli A. Keratinolytic potential of a novel Bacillus sp. P45 isolated from the Amazon basin fish Piaractus mesopotamicus. *International Biodeterioration & Biodegradation*. 2009;63(3):358–363.
12. Daroit DJ, Correa AP, Brandelli A. Production of keratinolytic proteases through bioconversion of feather meal by the Amazonian Bacterium Bacillus sp. P45. *International Biodeterioration & Biodegradation*. 2011;65(1):45–51.
13. Corrêa APF, Daroit DJ, Coelho J, et al. Antioxidant, antihypertensive and antimicrobial properties of ovine milk caseinate hydrolyzed with a microbial protease. *J Sci Food Agric*. 2011;91(12):2247–2254.
14. Hidalgo ME, Daroit DJ, Folmer AP, et al. Physicochemical and antioxidant properties of bovine caseinate hydrolysates obtained through microbial protease treatment. *International Journal of Dairy Technology*. 2012;65(3):342–352.
15. Foegeding EA. Rheology and sensory texture of biopolymer gels. *Current Opinion in Colloid & Interface Science*. 2007;12(4-5):242–250.
16. Sabadini E, Hubinger MD, Cunha RL. The effects of sucrose on the mechanical properties of acid milk proteins-k-carrageenan gels. *Braz J Chem Eng*. 2006;23(1):55–65.
17. Costa JP, et al. *Texture Analysis of Milk Protein Gels using Digital Image Analysis*. Bioinformatics, SciTePress; 2011.
18. Ingrassia R, Costa JP, Hidalgo ME, et al. Application of a digital image procedure to evaluate microstructure of caseinate and soy protein acid gels. *LWT - Food Science and Technology*. 2013;53(1):120–127.
19. Langton M, Hermansson AM. Image analysis of particulate whey protein gels. *Food Hydrocolloids*. 1996;10(2):179–191.
20. Zheng C, Sun D, Zheng L. Recent applications of image texture for evaluation of food qualities-a review. *Trends in Food Science & Technology*. 2006;17(3):113–128.

21. Hummel BCW, Schor JM, Buck FF, et al. Quantitative enzymic assay of human plasminogen and plasmin with azocasein as substrate. *Analytical Biochemistry*. 1965;11(3):532–547.

22. Kuaye AY. An ultraviolet spectrophotometric method to determine milk protein content in alkaline medium. *Food Chemistry*. 1994;49(2):207–211.

23. Risso P, et al. Efecto del calcio sobre la gelificación de micelas de caseína bovina por acción enzimática de la quimosina. XI Congreso Argentino de Ciencia y Tecnología de Alimentos (XI CYTAL), Buenos Aires; 2007.

24. Camerini-Otero RD, Day LA. The wavelength dependence of the turbidity of solutions of macromolecules. *Biopolymers*. 1978;17(9):2241–2249.

25. Horne DS. Determination of the fractal dimension using turbidimetric techniques. Application to aggregating protein systems. *Faraday Discussions of the Chemical Society*. 1987;83:259–270.

26. Risso P, Relling VM, Armesto MS, et al. Effect of size, proteic composition, and heat treatment on the colloidal stability of proteolyzed bovine casein micelles. *Colloid & Polymer Science*. 2007;285(7):809–817.

27. Mancilla Canales MA, Hidalgo ME, Risso PH, et al. Colloidal Stability of Bovine Calcium Caseinate Suspensions. Effect of Protein Concentration and the Presence of Sucrose and Lactose. *J Chem Eng Data*. 2010;55(7):2550–2557.

28. Montgomery DC. *Design and Analysis of Experiments*. John Wiley & Sons; 2006.

29. Arima K, et al. *Milk-clotting enzyme from Mucor pusillus var. Lindt*. Methods in Enzymology. GE Perlmann and L Lorand. New York: Academic Press. 1970;19:446–459.

30. Gonzalez RC, Woods RE. *Digital Image Processing*. Pearson/Prentice Hall; 2008.

31. Curcio S, Gabriele D, Giordano V, et al. A rheological approach to the study of concentrated milk clotting. *Rheologica Acta*. 2001;40(2):154–161.

32. Anema SG, Lee SK, Lowe EK, et al. Rheological Properties of Acid Gels Prepared from Heated pH- Adjusted Skim Milk. *Journal of Agricultural and Food Chemistry*. 2004;52(2):337–343.

33. Braga ALM, Menossi M, Cunha RL. The effect of the glucono-[delta]-lactone/caseinate ratio on sodium caseinate gelation. *International Dairy Journal*. 2006;16(5):389–398.

34. Re R, Pellegrini N, Anna P, et al. Antioxidant activity applying an improved ABTS radical cation decolorization assay. *Free Radical Biology and Medicine*. 1999;26(9-10):1231–1237.

35. Corrêa APF, Daroit DJ, Roberta F, et al. Hydrolysates of sheep cheese whey as a source of bioactive peptides with antioxidant and angiotensin-converting enzyme inhibitory activities. *Peptides*. 2014;61:48–55.

36. Oyaizu M. Studies on products of browning reaction antioxidative activities of products of browning reaction prepared from glucosamine. *The Japanese Journal of Nutrition and Dietetics*. 1986;44(6):307–315.

37. Zhu K, Zhou H, Qian H. Antioxidant and free radical-scavenging activities of wheat germ protein hydrolysates (WGPH) prepared with alcalase. *Process Biochemistry*. 2006;41(6):1296–1302.

38. de Castro Leite Júnior BR, LimaTribst AA, Cristianini M. Proteolytic and milk-clotting activities of calf rennet processed by high pressure homogenization and the influence on the rheological behavior of the milk coagulation process. *Innovative Food Science & Emerging Technologies*. 2014;21:44–49.

39. Blecker C, Habib-Jiwan JM, Karoui R. Effect of heat treatment of rennet skim milk induced coagulation on the rheological properties and molecular structure determined by synchronous fluorescence spectroscopy and turbiscan. *Food Chemistry*. 2012;135(3):1809–1817.

40. Clausen MR, Skibsted LH, Stagsted J. Characterization of Major Radical Scavenger Species in Bovine Milk through Size Exclusion Chromatography and Functional Assays. *Journal of Agricultural and Food Chemistry*. 2009;57(7):2912–2919.

41. Korhonen H. Milk-derived bioactive peptides: From science to applications. *Journal of Functional Foods*. 2009;1(2):177–187.

42. Conway V, Gauthier SF, Pouliot Y. Antioxidant Activities of Buttermilk Proteins, Whey Proteins, and Their Enzymatic Hydrolysates. *Journal of Agricultural and Food Chemistry*. 2013;61(2):364–372.

43. Tarango-Hernández S, Alarcón-Rojo AD, Robles-Sánchez M. et al. Potential of Fresco-style cheese whey as a source of protein fractions with antioxidant and Angiotensin-I-converting enzyme inhibitory activities. *J Dairy Sci*. 2015;98(11):7635–7639.

44. Hernández-Ledesma B, Miralles B, Amigo L, et al. Identification of antioxidant and ACE-inhibitory peptides in fermented milk. *Journal of the Science of Food and Agriculture.* 2005;85(6):1041–1048.

45. Silva SV, Malcata FX. Caseins as source of bioactive peptides. *International Dairy Journal*. 2005;15(1):1–15.